Vision Research Vol. 22, pp. 17 to 25, 1982
Printed in Great Britain

0042-6989/82/010017-09$03.00/0
Pergamon Press Ltd

SUMMATION OF GRATING PATCHES INDICATES MANY TYPES OF DETECTOR AT ONE RETINAL LOCATION*

ANDREW B. WATSON†
Physiological Laboratory, Cambridge University, Cambridge CB2 3EG, England

(*Received* 21 *August* 1980; *in revised form* 15 *June* 1981)

Abstract Summation between small, superimposed, fixated patches of sinusoidal grating of various spatial frequencies is explained by detectors with bandwidths of less than one octave. The smoothness of the local contrast sensitivity function indicates that detectors cannot be separated in frequency by more than one bandwidth. Together, these results suggest that the fovea is served by at least seven different frequency-selective detectors.

INTRODUCTION

It is well known that the visibility of a pattern depends upon its spatial distribution of contrast, and it is generally agreed that this is a consequence of the spatial selectivity of the detecting mechanism. Attempts to specify this selectivity, however, have shown that not one, but several independent and differently selective mechanisms are required (Campbell and Robson, 1968). The problem has thus become to define and enumerate these several mechanisms. Since all visual perception may derive from their outputs, the identity of these mechanisms is clearly a fundamental problem in vision.

Recent theories generally suppose a collection of many *detectors*, each with a linear spatial weighting function, some internal noise, and an output threshold (Limb and Rubinstein, 1977; Graham *et al.*, 1978; Quick *et al.*, 1978; Legge, 1978b; Wilson and Bergen, 1979; Robson and Graham, 1981). The weighting function of each detector, which may be likened to the receptive field sensitivity profile of a visual neuron, is centered upon a point in visual space. A pattern is detected whenever the integrated product of the stimulus and weighting function (their cross-correlation), plus noise, exceeds threshold in at least one detector.

An important issue in these theories is the number of detectors with different weighting functions that serve the same retinal area. Graham *et al.* (1978) have argued that since two small patches of sinusoidal grating which differ in frequency by a factor of three are detected independently, several types of detector must coexist at a given retinal location. Relying upon various measures of local spatial summation, Wilson and Bergen (1979), and Bergen *et al.* (1979) have claimed that only four different types of local detector are required. This report describes summation between small, superimposed, fixated patches of grating which differed in frequency by between 0.25 and 1.5 octaves. The results suggest at least seven different frequency-selective detectors at the fovea.

METHODS

Stimuli

In each session of the experiment, thresholds were measured concurrently for three stimuli: a patch of frequency f_1, a patch of frequency f_2, and a patch containing both frequencies f_1 and f_2. Examples of these stimuli are shown in Fig. 1.

In each stimulus, the luminance at a point x, y at time t is specified by

$$I(x,y,t) = I_0[1 + w(x,y,t)m(x)] \quad (1)$$

where I_0 is the mean luminance. The term $m(x)$ is the sum of the two horizontal sinusoidal components, of frequencies f_1 and f_2, and (pre-windowed) contrasts of c_1 and c_2,

$$m(x) = c_1\sin(2\pi f_1 x) + c_2\sin(2\pi f_2 x) \quad (2)$$

We define the *spread* of a Gaussian as the distance in which it falls from 1 to 1/e. The window function,

$$w(x,y,t) = \exp[-(x/s_x)^2 - (y/s_y)^2 - (t/s_t)^2] \quad (3)$$

is the product of horizontal, vertical, and temporal Gaussians, with spreads of s_x, s_y, and s_t. All three Gaussians were truncated at plus and minus two spreads. The temporal spread was always 250 msec. The horozontal and vertical spreads were always equal, and were set within each session to 1.5 periods of the lower of the two spatial frequencies used. Note that each sinusoidal component was always presented in sine phase relative to the center of the Gaussian.

* Some of these results were reported in April, 1980 at the meetings of the Association for Research in Vision and Ophthalmology (Watson, 1980).

† Present address: Department of Psychology, Building 420, Jordan Hall, Stanford University, Stanford, CA 94305.

The Gaussian window served to confine the stimuli in space time, as well as in spatial and temporal frequency. For example, the (positive) temporal frequency spectrum of each stimulus was Gaussian, centered on 0 Hz, with a half-amplitude bandwidth of 2.12 Hz. The (positive) spatial frequency spectrum of each stimulus is the sum of Gaussians centered on f_1 and f_2, with half-amplitude bandwidths of less than or equal to 0.52 octaves.

Experiment 1 measured summation between low spatial frequencies: f_1 was always 1 c/deg, and f_2 was either 1.189, 1.297, 1.414, 1.682, 2.000, 2.378 or 2.828 c/deg. Horizontal and vertical spreads were both 1.5 deg. In experiment 2, f_1 was always 16 c/deg, and f_2 was either 20.75, 22.60, 26.90, or 32.00 c/deg. Horizontal and vertical spreads were 3/32 deg.

The stimuli were generated by computer on a large (20 × 30 cm), bright (340 cd/m^2) CRT with a P-31 phosphor. The screen was surrounded by a 61 × 61 cm surface of about the same brightness, but somewhat lower saturation. Horizontal and temporal modulation were produced by conventional means (Graham *et al.*, 1978); to produce the vertical modulation, the product of the horizontal and temporal waveforms was multiplied, once during each unblanked cycle of the 100 KHz raster, by the output of a very fast buffer memory and digital-to-analog converter.

Viewing conditions

In Experiment 1, the viewing distance was 114 cm, and the patterns were centered on a tiny fixation point. For the smaller patches and higher spatial frequencies used in Experiment 2, viewing distance was 401 cm and the patterns were centered between two vertical and two horizontal 1 cm lines, their near ends separated by 3 cm (about 0.43 deg). All patterns were viewed binocularly with natural pupils by the author.

Experimental procedures

Thresholds were measured by a two-alternative, forced-choice QUEST staircase (Watson and Pelli, 1979). Threshold is defined as the contrast at which 82% of the responses are correct. On each trial, the stimulus is presented at the most probable estimate of its threshold contrast, as calculated from all previous trials. After a fixed number of trials, a final estimate of threshold was derived by a maximum likelihood method (Watson, 1979). In Experiment 1 each session contained 64 trials of each stimulus, in Experiment 2, 32 trials.

Within a session, thresholds were measured for a patch of frequency f_1, a patch of f_2, and a compound patch with components of both f_1 and f_2. Trials with the three types of stimuli were randomly intermixed. In each session, the ratio c_1/c_2 of the contrasts of the two components in the compound was fixed at the best estimate available at the start of the session of the ratio of the respective individual thresholds for the two components. Calculated predictions of a wide variety of models suggest that this generally insures the greatest possible amount of summation between the components.

RESULTS

The results of six sessions measuring summation between components of 1 and 2 c/deg are shown in Fig. 2. Let c_1^* and c_2^* be the average contrast thresholds for the f_1 and f_2 components alone. The abscissa specifies the contrast of the 1 c/deg component, divided by the average threshold contrast for the 1 c/deg patch alone, or c_1/c_1^*. The ordinate indicates the contrast of the 2 c/deg component, divided by the average threshold for that component, or c_2/c_2^*. The six estimates of threshold for 1 c/deg are on the abscissa, and those for 2 c/deg on the ordinate. The nearby arrows show ±1 SE.

The thresholds for the compound patches lie in the upper right of the graph. Since the contrast ratio of the two components was re-adjusted before each session, the points do not lie on a common ray from the origin. Hence there is no straightforward method of averaging these thresholds. However, a single measure of summation can be derived. Let c_1 and c_2 be the contrasts of the two components in a compound threshold. A parameter M (>0) defines a unique contour of the form

$$1 = (c_1/c_1^*)^M + (c_2/c_2^*)^M \quad (4)$$

which intersects the three points $(c_1^*, 0)$, $(0, c_2^*)$, and (c_1, c_2). The contours for two compounds are sketched in Fig. 2. These particular compounds give values of M of 2.10 and 5.95. If a contour of this form describes summation in the neighbourhood of the compound threshold and the 45 degree ray, then the intersection of the ray and the contour is an estimate of the threshold that would have been obtained had it been measured along the ray. At the intersection, the ratio of either component to compound threshold (c_1^*/c_1 or c_2^*/c_2, that is, the inverse of either coordinate) is $2^{1/M}$. Call this the *threshold ratio*†.

Complete summation, as when the two components are identical, will give a ratio of 2; the complete absence of summation will give a ratio of 1; probability summation between the two components will give a ratio of about 1.2 (Watson and Nachmias, 1980). The average of the threshold ratios of Fig. 2 is shown by the filled symbol.

Experiment 1

The average threshold ratios determined in Experiment 1 are plotted in Fig. 3 as a function of the frequency of the second component. The first com-

† In one case out of the 44 reported in this paper (the uppermost point in Fig. 2) M could not be estimated and was set arbitrarily to infinity, giving an intersection at (1, 1) and a threshold ratio of 1.

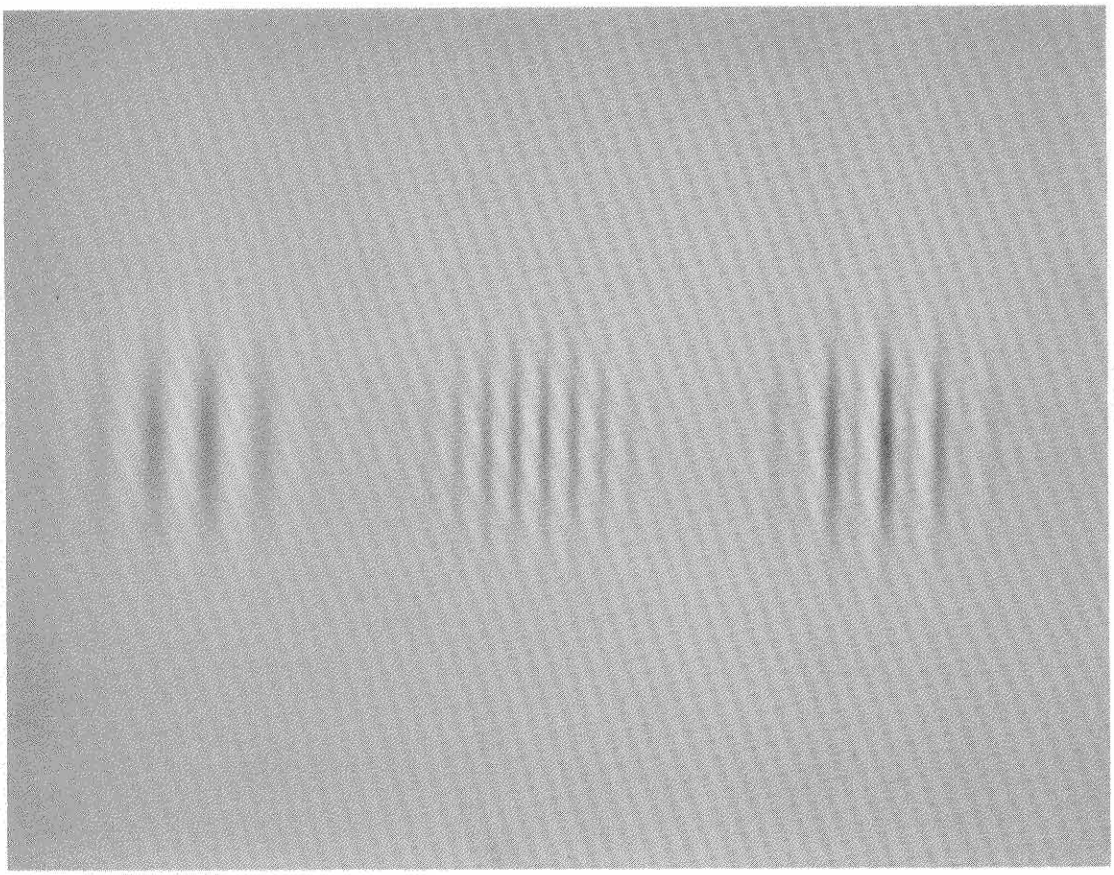

Fig. 1. From left to right: a patch of frequency f_1; a patch of frequency $f_2 = 2f_1$; a patch containing components of f_1 and f_2, added in sine phase with equal amplitudes. The horizontal and vertical spreads for all three patches are $1.5/f_1$.

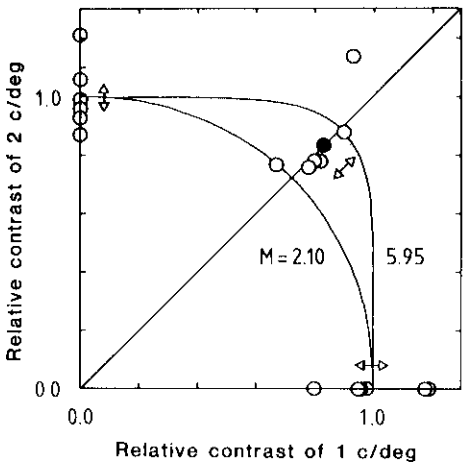

Fig. 2. Simple and compound thresholds from six sessions of Experiment 1. Component frequencies were 1 and 2 c/deg. The abscissa indicates contrast of the 1 c/deg component divided by the average of the six estimates of threshold for that component alone. Those estimates are plotted on the abscissa. The ordinate gives the contrast of the 2 c/deg component, divided by the average threshold for that component. Open symbols in the upper right are compound thresholds. The filled symbol is an estimate of the average compound threshold, as derived in the text. The arrows show ±1 SE. The smooth curves are equation 4 with M equal to 2.10 and 5.95.

ponent frequency was always 1 c/deg. Each point is the average of at least 3 sessions and the error bars show plus and minus one standard error. Note that the data in Fig. 2 are represented by the point at 2 c/deg.

Summation declines rapidly with increasing separation between the component frequencies, so that an octave away only an amount consistent with probability summation remains. The curves in this figure, and in Figs 4, 5 and 6, will be described below.

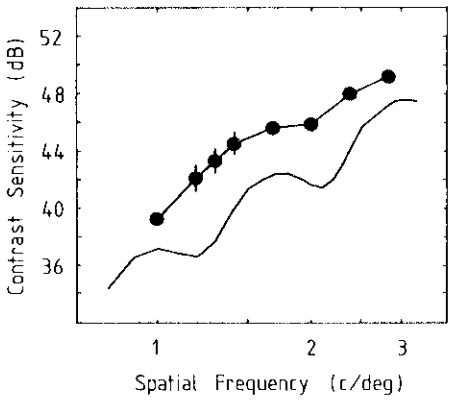

Fig. 4. Contrast sensitivities for simple patches from Experiment 1. Decibels are 20 times the log to the base 10. Plus and minus 1 SE are shown when larger than the symbol size. The lower curve is a model prediction described in the text.

The single component thresholds for all the frequencies used in Experiment 1 are plotted in Fig. 4. Where larger than the symbol size, plus and minus one standard error ar shown. The sensitivities are typical for spatio-temporal patterns of this sort.

Experiment 2

Figure 5 shows the average threshold ratios for compounds of 16 c/deg and the frequency noted on the abscissa. On the logarithmic abscissa used here, the decline in summation is very similar to that shown in Fig. 3. When separated by an octave, the two frequencies exhibit only probability summation. Figure 6 shows the single component thresholds of each of the frequencies used in Experiment 2.

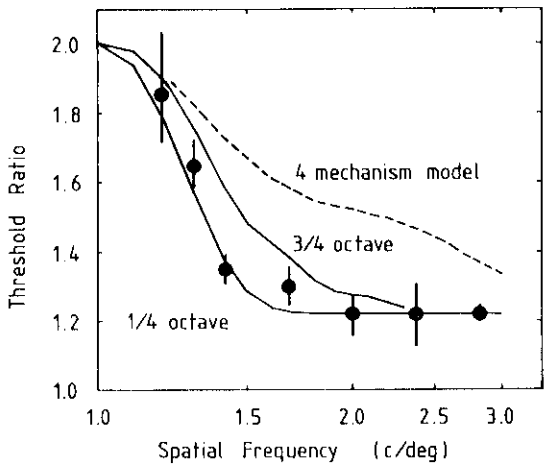

Fig. 3. The ratio of simple to compound thresholds from Experiment 1 for compounds of 1 c/deg and the frequency on the abscissa. The bars show ±1 SE. The solid and dashed curves are predictions of models described in the text.

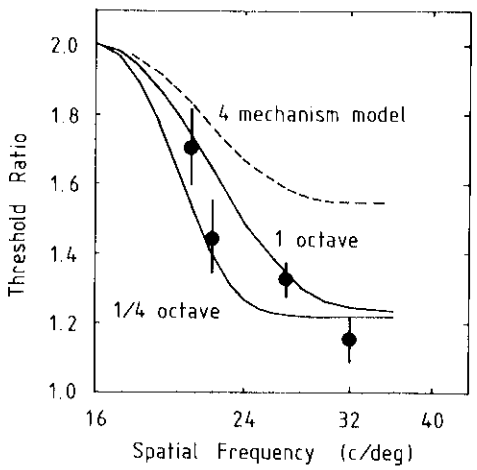

Fig. 5. Threshold ratios from Experiment 2 for compounds of 16 c/deg and the frequency on the abscissa. Details as in Fig. 3.

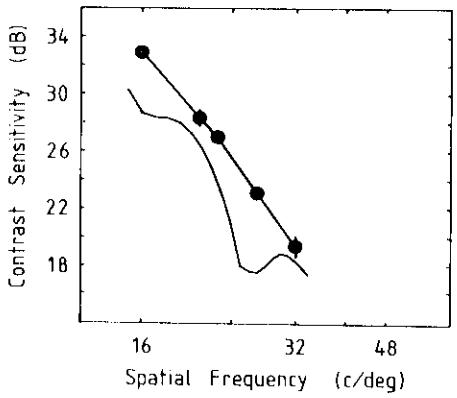

Fig. 6. Contrast sensitivities for simple patches from Experiment 2. Details as in Fig. 4.

THE FOUR-MECHANISM MODEL

Wilson and Bergen (1979) have proposed a model of threshold spatial vision which contains just four different sized detectors at each eccentricity. The model has been described in sufficient quantitative detail that it is possible to calculate predictions for the data reported here. These are shown by the dashed lines in Figs 3 and 5. The parameters used were those published for observer H.R.W. under "sustained" modulation. For both the low and high ranges of spatial frequency, the model predicts substantially more summation than is found. Wilson and Bergen note that their model is intended to deal only with frequencies between 0.25 and 16 c/deg, and so contains only one mechanism above 16 c/deg. Thus the prediction in Fig. 5 is effectively that of a single mechanism. The failure of this prediction suggests the need for additional detectors above 16 c/deg. Marr *et al.* (1980) arrive at a similar conclusion from consideration of various acuity measurements.

The model also fails to predict the threshold ratios of Experiment 1, which used frequencies within the range considered by the model. Bergen *et al.* (1979) have also measured summation between frequency components in this range, and find them to be explained by the four-mechanism model. The substantial differences in method between their experiments and those reported here may explain this discrepancy, but it is clear that the four-mechanism model does not describe the present data.†

THE FREQUENCY-PATCH DETECTOR MODEL

The four-mechanism model predicts more summation than is found. This suggests that the detectors in that model have too large a bandwidth (about 1.75 octaves). As an alternative, I have considered a model in which the bandwidth is treated as a free parameter.

The model resembles in several respects a version considered by Quick *et al.* (1978), which in turn embodied elements of many previous models. In essence it is a collection of many statistically-independent, frequency-selective detectors distributed over visual space. Since each detector responds to a particular band of spatial frequency within a patch of visual space, the model has been called the *frequency-patch detector*. A more detailed description follows.

Detector weighting function

Each detector has a weighting function defined by the product of a Gaussian function and either a cosine or a sine function. These form symmetric and antisymmetric detectors, respectively. For example, the antisymmetric detector of frequency f_i has a weighting function

$$w_i(x) = \exp[-(xf_i/b)^2] \sin[2\pi f_i x], \quad (5)$$

where b is the spread of the Gaussian, expressed in periods of the detector frequency. A sketch of this weighting function, with b equal to 1.0, is shown in Fig. 7a.

The amplitude spectrum of this detector is approximately Gaussian, with a spread equal to $f_i/(\pi b)$. It is drawn in Fig. 7b. The half-amplitude bandwidth in octaves is

$$\log_2[(\pi b + \sqrt{\ln 2})/(\pi b - \sqrt{\ln 2})] \quad (6)$$

In the example shown, the bandwidth is 0.78 octaves. The quantity b is assumed to be constant for all detectors, so the octave bandwidth of all detectors is likewise constant. Support for this assumption will be given below.

All predictions shown assume both symmetric and antisymmetric detectors. Provided the spatial sampling interval is small enough (see below), one or the other of these classes may be omitted without substantially altering the results.

This shape of weighting function was chosen in part for theoretical convenience, since it permits easy manipulation of bandwidth and confines detector sensitivity in both space and spatial frequency, and in part for its resemblance to the spatial weighting functions of individual cortical neurons (e.g. Movshon *et al.*, 1978a; De Valois *et al.*, 1978). It is also important to note that functions like Equation 5 form a set of elementary signals into which an arbitrary function may be resolved (Gabor, 1946; Helstrom, 1966). Like the points or sinusoids used in the space or frequency description of a signal, these functions provide a complete and exact representation. Their unique property is that, unlike points or sinusoids, they are maximally localized in both space and frequency. The precise significance of this property for vision is not clear, but the limited space and frequency bandwidths of vision

† Among the differences in method between the present experiments and those of Bergen *et al.* (1979) are: (1) mean luminance of 340 cd/m^2 vs 7.8 cd/m^2; (2) Gaussian vs rectangular vertical window; (3) Gaussian vs no horizontal window; (4) equal contrast of components relative to their thresholds vs twice as much relative contrast in one component as in the other.

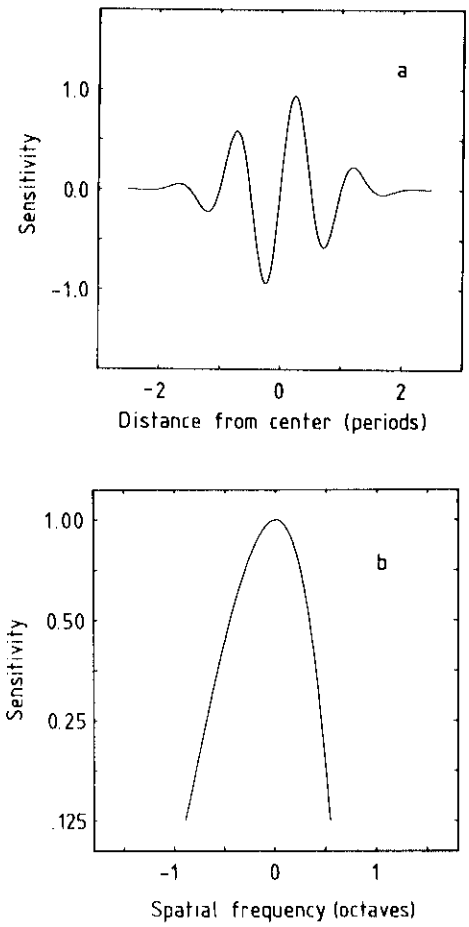

Fig. 7. (a) Weighting function of an antisymmetric detector in the frequency-patch detector model with $b = 1$. (b) Normalized amplitude spectrum of the detector. The bandwidth is 0.78 octaves.

may be noted. Marčelja (1980) has recently noted the resemblance of simple cortical cell receptive field profiles to the Gabor functions.

Spatial sampling interval

Each detector is located some distance x_{ij} from the fovea, thus

$$w_{ij}(x) = w_i(x - x_{ij}). \tag{7}$$

The array of detectors which share a common frequency f_i form a *channel*. A given channel will respond to frequency components lying within a certain band. To transmit these components without distortion, they must be sampled sufficiently often over space. If the highest frequency considered is that at which detector sensitivity is 10% of its maximum, then the separation between detectors should be

$$x_{ij+1} - x_{ij} = 1/[2f_i(1 + 1.52/(\pi b))] \tag{8}$$

As an example, the detectors in Fig. 7 would be placed at intervals of 0.34 of a period. This formula has been used in the calculations shown. Increasing the sample density above this level has very little effect.

Frequency sampling interval

Since detector bandwidths are a constant size on a log scale, it makes sense to sample the frequency spectrum at constant intervals on a log scale. Furthermore, since the sampling interval must also be made smaller as the bandwidth decreases, it is sensible to express this log frequency interval as a fraction of the detector bandwidth. In the calculations in Figs 3 and 5 the frequency sampling interval was 1/2 bandwidth. Smaller intervals give nearly identical results, while larger intervals will be shown to be incompatible with the data in Figs 4 and 6.

Detector sensitivity

The goal of this model is the prediction of relative, rather than absolute thresholds. However, the absolute thresholds of the detectors as a function of frequency or eccentricity can influence summation (Quick *et al.*, 1978). Since the stimuli used cover only small regions of space or frequency, these effects are likely to be modest, but they have nevertheless been taken into account.

The spatial variation in detector sensitivity has been represented by a decline of 3/8 of a decibel (1 dB = 1/20 log unit) per period of distance from the fovea, consistent with the data of Robson and Graham (1980). Declines of between 0 and 1 dB/period give very similar results.

The sensitivity of each channel has been adjusted so that the model approximately predicts the measured single patch thresholds. If the adjustment at frequency f_i is a_i, then the response of the detector at x_{ij} is scaled by

$$r_{ij} = a_i 10^{-f_i|x_{ij}|/3.3} \tag{9}$$

Detector response

Each detector responds in proportion to the cross-correlation of its weighting function and the stimulus waveform. If the stimulus is $f(x)$, then the response is

$$r_{ij} = r_{ij} \int_{-s}^{s} w_{ij}(x) f(x)\, dx. \tag{10}$$

Probability summation

We assume that uncorrelated noise is added to the response of each detector. Whenever the noisy response magnitude exceeds the output threshold, the detector "detects". The probability of this event increases with the magnitude of the response in the manner suggested by Brindley (1960) and Quick (1974).

$$p_{ij} = 1 - \exp[-|r_{ij}|^{\beta}] \tag{11}$$

where β controls the rate of increase.

The observer makes a correct forced-choice response when at least one detection occurs, or when he

guesses correctly. The psychometric function is then

$$p = 1 - 0.5 \prod_i \prod_j (1 - p_{ij}) \quad (12)$$

$$= 1 - 0.5 \exp\left[- \sum_i \sum_j |r_{ij}|^\beta \right]. \quad (13)$$

Hence for all stimuli at threshold, defined in these experiments as $p = 0.82$,

$$1 = \sum_i \sum_j |r_{ij}|^\beta. \quad (14)$$

The exponent β has been taken to be 3.5, consistent with the psychometric functions collected in this and a wide variety of other experiments. This formulation of the effects of probability summation has been found to give a good account of sensitivity to stimuli extended in spatial frequency, space, and time (Graham *et al.*, 1978; Legge, 1978a, b; Watson, 1979; Robson and Graham, 1980; Watson and Nachmias, 1980; Watson *et al.*, 1980).

Only detectors whose weighting functions overlap the stimulus in both space and spatial frequency need be considered, since in all others the probability of detection will be zero.

Dimensions neglected by the model

The model considers the stimuli only in the horizontal spatial dimension. It is probable that detectors are also selective in the vertical spatial dimension, as well as in orientation, temporal frequency, wavelength, direction of motion, and so on. Furthermore, these selectivities may not be orthogonal, so that a particular selectivity in one dimension may entail selectivity in another. It is possible that in neglecting other dimensions we may attribute too much selectivity to the detectors in the dimension of horizontal spatial frequency. The fact that the stimuli were constant and compact in their other dimensions, however, will minimize any error of this sort.

MODEL PREDICTIONS

Summation vs bandwidth

The two solid curves in Fig. 3 are predictions of the frequency-patch model when each detector has a bandwidth of 1/4 or 3/4 octaves. The curves bracket the data, giving upper and lower bounds on the detector bandwidth. A good fit by eye is given by 1/2 octave detectors.

The solid curves in Fig. 5 show the predictions of bandwidths of 1/4 and 1 octaves. The 3/4 octave prediction (not shown) is somewhat below that in Fig. 3, a consequence of the adjustment of detector sensitivities. A bandwidth of 1/2 octave gives a good fit to these data as well.

As noted above, the predicted thresholds for compound patches are remarkably resistant to variations in all model parameters save the detector bandwidth. To account for the data, the detectors must have bandwidths of less than 3/4 octave at 1 c/deg, and less than 1 octave at 16 c/deg. Since bandwidths are nearly constant on a log scale, we may take 1 octave as an overall upper bound, and 1/2 octave as a rough overall best estimate of this property of the detectors.

Sensitivity vs frequency sampling interval

The detector bandwidth places an upper bound on the frequency sampling interval. The interval cannot be larger than a certain proportion of the bandwidth, or gaps will exist in the overall contrast sensitivity function of the model. This is illustrated by the lower curves in Figs 4 and 6, which show the sensitivity to patches predicted when the interval is a full bandwidth. The curves have been displaced downwards for clarity. The large undulations in predicted sensitivity are the result of the large interval used, and are absent when the interval is 1/2 bandwidth. Since it is very unlikely that still larger undulations would go undetected in the measured sensitivities, one full bandwidth appears to be an upper limit to the frequency sampling interval.

DISCUSSION

Number of detectors

If detector bandwidths are no larger than 1 octave, and the frequency sampling interval no larger than 1 bandwidth, then the range of frequency between 1 and 32 c/deg must be served at the fovea by no fewer than 6 different frequency selective detectors. An additional five sessions showed only probability summation (threshold ratio = 1.21) between patches of 0.25 and 0.75 c/deg, indicating the existence of at least one further mechanism.

If, as is consistent with the data, bandwidths are 3/4 octave, and the frequency sampling interval 1/2 bandwidth, then the fovea of this observer would require about 20 different frequency-selective detectors.

The data reported here were collected from one observer, the author. The use of a two-alternative forced-choice method and the mixing of single-component and compound patches within a session largely eliminate the possibility of observer bias, but the possibility of differences among observers remains. Quick *et al.* (1978) found some differences between observers in their measures of grating summation, but used the method of adjustment which is notoriously sensitive to the observer's criterion (Kelly and Savoie, 1973). While there is no *a priori* reason to expect differences between observers when a forced-choice method is used, caution requires that the conclusions above be drawn only about the single observer examined.

Physiological considerations

It is interesting to consider whether any physiologically identified class of visual neuron might satisfy the assumptions that define the detectors of the frequency-patch model. The X and Y cells of the cat retina have each been shown to be uniformly sized at

any one eccentricity, thus providing only two frequency-selective detectors at each location (Peichl and Wassle, 1979; Cleland *et al.*, 1979). But we know very little about the 30–70% of ganglion cells that are neither X nor Y (Peichl and Wassle, 1979). A stronger objection to the ganglion cells is their large bandwidth. This measure depends somewhat on experimental conditions, but is rarely less than 2 octaves. The same objection applies to cells of the lateral geniculate nucleus (Derrington and Fuchs, 1979).

In the cortex of the cat, the results of Movshon *et al.* (1978c) suggest that few of the cells in area 18 would respond to the very slow time course of the stimuli used here. If there is a functional homolog to this area in the human, presumably it is also insensitive.

However, cells in area 17 of the cat respond well to the low temporal frequencies used here (Movshon *et al.*, 1978c). Unlike the frequency-patch detectors, the complex cells show gross non-linearities of spatial summation (Movshon *et al.*, 1978b). They may nevertheless detect the stimuli used here, and a model incorporating such elements might account for the present results. On the other hand, simple cells in both cat and monkey show linear spatial summation followed by an output threshold (Movshon *et al.*, 1978a; De Valois *et al.*, 1978). In the cat, simple cells at one eccentricity are tuned to frequencies ranging over as much as three octaves (Movshon *et al.*, 1978c). Though in both sepecies frequency bandwidths vary considerably from cell to cell, Movshon *et al.* (1978c) found 15% of simple cells in area 17 in the cat had bandwidths of less than 1 octave. Albrecht *et al.* (1980) report a slightly higher percentage (but averaged unspecified numbers of simple and complex cells from both cat and monkey). Hence by virtue of their bandwidths, variety of tuning at one eccentricity, sensitivity to slow variation in time, linearity of spatial summation, and output thresholds, the simple cells in area 17 of the cat, and perhaps monkey, might provide a physiological basis for the frequency-patch detector model.

Acknowledgements—Support for this work was provided by NIH postdoctoral fellowship F32-EY05219 to the author. I thank John Robson for the use of his equipment and ideas.

REFERENCES

Albrecht D. G., De Valois R. L. and Thorell L. G. (1979) Visual cortical neurons: are bars or gratings the optimal stimuli? *Science* **207,** 88–90.

Bergen J. R., Wilson H. R. and Cowan J. D. (1979) Further evidence for four mechanisms mediating vision at threshold: Sensitivities to complex gratings and aperiodic stimuli. *J. opt. Soc. Am.* **69,** 1580–1587.

Brindley G. S. (1960) *Physiology of the Retina and Visual Pathway*, p. 192. Edward Arnold, London.

Campbell F. W. and Robson J. G. (1968) Application of Fourier analysis to the visibility of gratings. *J. Physiol., Lond.* **197,** 551–566.

Cleland B. G., Harding T. H. and Tulunay-Keesey U. (1979) Visual resolution and receptive field size: Examination of two kinds of cat retinal ganglion cell. *Science* **205,** 1015–1017.

Derrington A. M. and Fuchs A. F. (1979) Spatial and temporal properties of X and Y cells in the lateral geniculate nucleus. *J. Physiol., Lond.* **293,** 347–363.

De Valois R. L., Albrecht D. G. and Thorell L. G. (1978) Cortical cells: bar and edge detectors, or spatial frequency filters. In *Frontiers of Visual Science* (Edited by Cool S. J. and Smith E. L.), pp. 544–556. Springer, New York.

Gabor D. (1946) Theory of Communication. *J. IEE London*, **93(III),** 429–457.

Graham N., Robson J. G. and Nachmias J. (1978) Grating summation in fovea and periphery. *Vision Res.* **18,** 815–825.

Helstrom C. W. (1966) An expansion of a signal in Gaussian elementary signals. *IEEE Trans. Inf. Theory* **IT-13,** 81–82.

Kelly D. H. and Savoie R. E. (1973) A study of sine-wave contrast sensitivity by two psychophysical methods. *Percept. Psychophys.* 14, 313–318.

Legge G. E. (1978a) Sustained and transient mechanisms in human vision: temporal and spatial properties. *Vision Res.* **18,** 69–81.

Legge G. E. (1978b) Space domain properties of a spatial frequency channel in human vision. *Vision Res.* **18,** 959–969.

Limb J. O. and Rubinstein C. B. (1977) A model of threshold vision incorporating inhomogeneity of the visual field. *Vision Res.* **17,** 571–584.

Marčelja S. (1980) Mathematical description of the responses of simple cortical cells. *J. opt. Soc. Am.* **70,** 1297–1300.

Marr D., Poggio T. and Hildreth E. (1980) Smallest channel in early human vision. *J. opt. Soc. Am.* **70,** 868–870.

Movshon J. A., Thompson I. D. and Tolhurst D. J. (1978a) Spatial summation in the receptive fields of simple cells in the cat's striate cortex. *J. Physiol., Lond.* **283,** 53–77.

Movshon J. A., Thompson I. D. and Tolhurst D. J. (1978b) Receptive field organization of complex cells in the cat's striate cortex. *J. Physiol., Lond.* **283,** 79–99.

Movshon J. A., Thompson I. D. and Tolhurst D. J. (1978c) Spatial and temporal contrast sensitivity of neurones in areas 17 and 18 of the cat's visual cortex. *J. Physiol., Lond.* **283,** 101–120.

Peichl L. and Wassle H. (1979) Size, scatter, and coverage of ganglion cell receptive field centers in the cat retina. *J. Physiol., Lond.* **291,** 117–141.

Quick R. F. Jr (1974) A vector-magnitude model of contrast detection. *Kybernetik* **16,** 65–67.

Quick R. F. Jr, Mullins W. W. and Reichert T. A. (1978) Spatial summation effects on two-component grating thresholds. *J. opt. Soc. Am.* **68,** 116–121.

Robson J. G. and Graham N. (1981) Probability summation and regional variation in contrast sensitivity across the visual field. *Vision Res.* **21,** 409–418.

Watson A. B. (1979) Probability summation over time. *Vision Res.* **19,** 515–522.

Watson A. B. (1980) Summation of grating patches implies many frequency-selective detectors at one retinal location. *Invest. Ophthal. visual Sci.* Suppl, **19,** 45.

Watson A. B. and Nachmias J. (1980) Summation of asynchronous gratings. *Vision Res.* **20,** 91–94.

Watson A. B., Thompson P. G., Murphy B. J. and Nachmias J. (1980) Summation and discrimination of gratings moving in opposite directions. *Vision Res.* **20,** 341–347.

Watson A. B. and Pelli D. G. (1979) The QUEST staircase procedure. *Appl. Vision Assoc. Newslett.* **14,** 6–7.

Wilson H. R. and Bergen J. R. (1979) A four mechanism model for threshold spatial vision. *Vision Res.* **19,** 19–33.